BI-TP 95/31
hep-ph/9510386

On the Observation of Bosonic Loop Corrections in Electroweak Precision Experiments †

S. Dittmaier, D. Schildknecht and G. Weiglein‡

Fakultät für Physik, Universität Bielefeld, Germany

Abstract

We investigate the structure of the experimentally significant electroweak bosonic loop corrections to the leptonic weak mixing angle, the leptonic Z-boson decay width, and the W-boson mass. It is shown that the bosonic corrections that have a sizable effect at the present level of experimental accuracy are directly related to the use of the Fermi constant G_μ as input parameter for analyzing the LEP observables. Indeed, if the (theoretical value of the) leptonic width of the W boson is used as input parameter instead of the low-energy parameter G_μ determined from muon decay, fermion-loop corrections are sufficient for compatibility between theory and experiment.

October 1995

†Partially supported by the EC-network contract CHRX-CT94-0579.

‡Supported by the Bundesministerium für Bildung und Forschung, Bonn, Germany.

1 Introduction

The data taken at the Z-boson resonance at LEP1 and the determination of the W-boson mass provide the most stringent test of the electroweak Standard Model (SM) at present. As previously emphasized [1], genuine precision tests of the electroweak theory require an experimental accuracy that allows to distinguish between the pure fermion-loop and the full one-loop predictions of the theory. This accuracy was first reached in 1994. Indeed, by systematically discriminating between fermion-loop (vacuum-polarization) corrections to the photon, Z- and $W^{\pm}$-boson propagators and the full one-loop results, it was found [2, 3] that contributions beyond fermion loops are required for consistency with the experimental results on the leptonic Z-peak observables and the W-boson mass. While the pure fermion-loop predictions were shown to be incompatible with the data on the leptonic Z-boson decay width Γ_{l}, the effective weak mixing angle $\bar{s}_{\mathrm{W}}^2$, and $M_{\mathrm{W}^{\pm}}$, the complete one-loop prediction of the SM provides a consistent description of the experimental results. Consequently, the data have become sensitive to the non-Abelian gauge structure of the standard electroweak theory entering the bosonic radiative corrections.

The investigations performed in Refs. [2, 3] differ from related work [4] that is concerned with the evidence for radiative corrections beyond the $\alpha(M_{\mathrm{Z}}^2)$-Born approximation. While the $\alpha(M_{\mathrm{Z}}^2)$-Born approximation contains fermion-loop corrections to the photon propagator only, in Refs. [2, 3] the full fermion-loop predictions are compared with the experimental data and the complete SM result, thus exploring the nature of the electroweak loop corrections and revealing that in fact *bosonic* electroweak corrections are required for consistency with the data. The experimental evidence for bosonic loop corrections was also explored for the single observable $\bar{s}_{\mathrm{W}}^2$ in Ref. [5] and for $M_{\mathrm{W}^{\pm}}$ in Ref. [6].

The necessity of taking into account standard bosonic corrections for consistency with the data thus being established, it is desirable to explore the detailed structure of those bosonic corrections to which the experiments are actually sensitive. This is the topic of the present article. In order to investigate the structure of the radiative corrections it is convenient to employ a suitable set of effective parameters. In Ref. [2] three effective parameters, Δx, Δy, and ε, have been used to accommodate the radiative corrections to the observables Γ_{l}, $\bar{s}_{\mathrm{W}}^2$, and $M_{\mathrm{W}^{\pm}}$. These parameters quantify possible sources of SU(2) violation in the framework of an effective Lagrangian [7] for electroweak interactions. They are directly related to observables and are thus manifestly gauge-independent quantities. This analysis was extended in Ref. [3] by including also the hadronic decay modes of the Z boson. It has been shown that the experimentally resolved bosonic corrections are entirely contained in the single parameter Δy (corresponding to ε_2 in the notation of Ref. [8]), which in turn is extremely insensitive to variations in the Higgs-boson mass.

The parameter Δy relates the effective charged-current coupling, $g_{\mathrm{W}^{\pm}}(0)$, determined from muon decay via the Fermi constant G_{μ}, to its neutral-current counterpart, $g_{\mathrm{W}^0}(M_{\mathrm{Z}}^2)$, appearing in Z-boson decay. Thus, Δy quantifies isospin breaking between the neutral-current and charged-current interactions as well as the transition from the low-energy process muon decay to the energy scale of the LEP1 observables, i.e. the Z-boson mass.

The isospin-breaking effect in the $(W^{\pm}, W^0)$ triplet will be studied in Sect. 2 of the present paper by relating Z-boson decay to $W^{\pm}$-boson decay. It will be shown that the bosonic contribution to the isospin-breaking effect is small in the standard electroweak

theory when compared with present (and even future) experimental accuracy. As a consequence, the bosonic corrections significant for the current precision experiments are related to the transition from the charged-current coupling $g_{W^\pm}(0)$ defined via muon decay to the charged-current coupling at the scale of the W-boson mass, $g_{W^\pm}(M^2_{W^\pm})$, being deduced from the W-boson decay width into leptons. It will be demonstrated that it is indeed sufficient to combine the fermion-loop predictions with the bosonic contribution furnishing the transition from $g_{W^\pm}(0)$ to $g_{W^\pm}(M^2_{W^\pm})$ in order to achieve agreement between theory and experiment. The quality of this approximation is illustrated not only at the level of the effective parameters but also directly for the leptonic LEP1 observables and the W-boson mass.

In Sect. 3 it will be shown that the occurrence of the experimentally relevant bosonic corrections could completely be avoided by introducing the W-boson decay width as input parameter for analyzing the precision data instead of the low-energy quantity G_μ. Using the SM theoretical value of the leptonic W-boson width as input, it will explicitly be demonstrated that omission of the standard bosonic corrections to the LEP1 observables and the W-boson mass does not lead to a significant deviation between theory and experiment. Final conclusions are drawn in Sect. 4. The appendix provides some auxiliary formulae.

2 Scale-change and isospin-breaking contributions to the parameter Δy

2.1 Definitions

We work with the effective Lagrangian $\mathcal{L} = \mathcal{L}_C + \mathcal{L}_N$ for LEP1 observables introduced in Refs. [2, 3, 7]. In the leptonic sector SU(2)-breaking effects are quantified by the parameters x, y, ε. More precisely, x is defined as the mass ratio in the $(W^\pm, W^0)$ triplet,

$$M^2_{W^\pm} = x M^2_{W^0} = (1 + \Delta x) M^2_{W^0}, \tag{1}$$

y as the ratio of the effective $W^\pm$ and W^0 couplings to charged leptons,

$$g^2_{W^\pm}(0) = y g^2_{W^0}(M^2_Z) = (1 + \Delta y) g^2_{W^0}(M^2_Z), \tag{2}$$

and ε quantifies SU(2) violation in γW^0 mixing,

$$\mathcal{L}_{\rm mix} = -\frac{1}{2}\frac{e(M^2_Z)}{g_{W^0}(M^2_Z)}(1 - \varepsilon) A_{\mu\nu} W^{0,\mu\nu}. \tag{3}$$

In this section we focus on the parameter y, which is the only one incorporating significant bosonic corrections. The charged-current Lagrangian $\mathcal{L}_C$ has the form

$$\mathcal{L}_C = -\frac{1}{2} W^{+\mu\nu} W^-_{\mu\nu} - \frac{g_{W^\pm}}{\sqrt{2}} \left(j^+_\mu W^{+\mu} + h.c. \right) + M^2_{W^\pm} W^+_\mu W^{-\mu}. \tag{4}$$

In Refs. [2, 3, 7] the charged-current coupling $g_{W^\pm}$ in (4) was defined with respect to muon decay, i.e. at a low-energy scale, as

$$g^2_{W^\pm}(0) \equiv 4\sqrt{2} G_\mu M^2_{W^\pm}. \tag{5}$$

The choice of the low-energy quantity $g_{\mathrm{W}^\pm}(0)$ is of course dictated by the fact that G_μ is the most accurately known electroweak parameter apart from the LEP observables to be analyzed. According to (2), the parameter Δy describes both the transition from the charged-current to the neutral-current sector and the change from the low-energy process muon decay to the energy scale of the LEP observables.

The effective coupling of the W^0 field to charged leptons, $g_{\mathrm{W}^0}(M_{\mathrm{Z}}^2)$, is derived from Z-boson decay, i.e. from the neutral-current process where all associated particles are physical (on-shell). In order to separately study the effect of the isospin-breaking transition to the charged-current sector, one therefore has to consider the corresponding (charged-current) process of the isospin partner of the W^0 field, namely leptonic decay of the $\mathrm{W}^\pm$ boson. Accordingly, we introduce the charged-current coupling at the W-boson mass shell, $g_{\mathrm{W}^\pm}(M_{\mathrm{W}^\pm}^2)$, which is derived from the leptonic width $\Gamma_{\mathrm{l}}^{\mathrm{W}}$ of the W boson,

$$g_{\mathrm{W}^\pm}^2(M_{\mathrm{W}^\pm}^2) \equiv \frac{48\pi}{M_{\mathrm{W}^\pm}}\Gamma_{\mathrm{l}}^{\mathrm{W}}\left(1 + c_0^2\frac{3\alpha}{4\pi}\right)^{-1}, \tag{6}$$

where c_0^2 is defined [7] according to

$$c_0^2 s_0^2 \equiv c_0^2(1 - c_0^2) = \frac{\pi\alpha(M_{\mathrm{Z}}^2)}{\sqrt{2}G_\mu M_{\mathrm{Z}}^2}. \tag{7}$$

In analogy to (2) we relate $g_{\mathrm{W}^\pm}(M_{\mathrm{W}^\pm}^2)$ to $g_{\mathrm{W}^0}(M_{\mathrm{Z}}^2)$ by a parameter Δy^{IB},

$$g_{\mathrm{W}^\pm}^2(M_{\mathrm{W}^\pm}^2) = y^{\mathrm{IB}} g_{\mathrm{W}^0}^2(M_{\mathrm{Z}}^2) = (1 + \Delta y^{\mathrm{IB}}) g_{\mathrm{W}^0}^2(M_{\mathrm{Z}}^2), \tag{8}$$

where the index "IB" refers to weak "isospin-breaking". In (6) we have introduced a factor $(1 + c_0^2 3\alpha/(4\pi))$ by convention. It is related to the convention chosen in the treatment of the photonic corrections to the leptonic Z-boson decay width Γ_{l} [2, 3, 7]. The photonic contributions to Γ_{l} are pure QED corrections giving rise to a factor $(1 + 3\alpha/(4\pi))$ that is split off and not included in Δx, Δy, and ε. For the decay of the W boson, however, it is not possible to uniquely separate the QED contribution from the other one-loop corrections. As isospin breaking is associated with electromagnetic interactions, a meaningful definition of Δy^{IB} requires to treat the photonic corrections on the same footing in both the neutral and charged vector boson decay. One possibility to achieve this would be to include all photonic contributions into the bosonic corrections both for Z-boson and W-boson decay. Equivalently, as far as the magnitude of Δy^{IB} is concerned, one may keep the convention for the correction factor $(1 + 3\alpha/(4\pi))$ in the leptonic Z-boson decay width Γ_{l} and split off the corresponding factor also in the decay width of the W boson, $\Gamma_{\mathrm{l}}^{\mathrm{W}}$. This is the procedure adopted in (6). The appearance of c_0^2 in the correction factor in the W-boson decay width is due to the rotation in isospin space relating the physical field Z to the field W^0 entering the SU(2) isotriplet. Numerically the correction term introduced in (6) amounts to $c_0^2 3\alpha/(4\pi) = 1.3 \times 10^{-3}$. Even though the introduction of this correction term in (6) is well justified, it is worth noting that a different treatment of the photonic corrections, such as omission of the correction factor in (6), would only lead to minor changes that would not influence our final conclusions at all.

In the language of our effective Lagrangian (4), the transition from the charged-current coupling at the scale of the muon mass, $g_{\mathrm{W}^\pm}^2(0)$, to the charged-current coupling obtained

from the decay of the W boson into leptons, $g^2_{\mathrm{W}^\pm}(M^2_{\mathrm{W}^\pm})$, is denoted as a scale change effect and is expressed by a parameter Δy^{SC},

$$g^2_{\mathrm{W}^\pm}(0) = y^{\mathrm{SC}} g^2_{\mathrm{W}^\pm}(M^2_{\mathrm{W}^\pm}) = (1+\Delta y^{\mathrm{SC}}) g^2_{\mathrm{W}^\pm}(M^2_{\mathrm{W}^\pm}), \tag{9}$$

where the index "SC" means "scale change". Inserting (8) into (9) and comparing with (2), one finds that in linear approximation the parameter Δy is split into two additive contributions,

$$\Delta y = \Delta y^{\mathrm{SC}} + \Delta y^{\mathrm{IB}}, \tag{10}$$

which furnish the transition from $g^2_{\mathrm{W}^\pm}(0)$ to $g^2_{\mathrm{W}^\pm}(M^2_{\mathrm{W}^\pm})$ and from $g^2_{\mathrm{W}^\pm}(M^2_{\mathrm{W}^\pm})$ to $g^2_{\mathrm{W}^0}(M^2_{\mathrm{Z}})$, respectively. Upon substituting (5) and (6) in (9), one finds

$$\Delta y^{\mathrm{SC}} = \frac{M^3_{\mathrm{W}^\pm} G_\mu}{6\sqrt{2}\pi \Gamma^{\mathrm{W}}_{\mathrm{l}}} - 1 + c_0^2 \frac{3\alpha}{4\pi}, \tag{11}$$

which allows to determine Δy^{SC} (and consequently also Δy^{IB} from Δy according to (10)) both experimentally and theoretically.

In our analysis of the observables Γ_{l}, $\bar{s}^2_{\mathrm{W}}$, and $M_{\mathrm{W}^\pm}$, which are measured at the LEP energy scale, the influence of the low-energy input parameter G_μ determined from muon decay is localized in the single effective parameter Δy^{SC}. In an investigation performed directly at the level of the observables, on the other hand, the effect of using this low-energy input parameter for analyzing high-energy observables cannot be separated from the other corrections.

The phrase "scale change" used for Δy^{SC} should not be confused with an ordinary "running" of universal (propagator-type) contributions. The couplings $g_{\mathrm{W}^\pm}(0)$ and $g_{\mathrm{W}^\pm}(M^2_{\mathrm{W}^\pm})$, being defined with reference to muon decay and W-boson decay, respectively, are obviously process-dependent quantities. While the fermion-loop contributions to Δy^{SC} are of propagator-type, the bosonic contributions to Δy^{SC} contain self-energy, vertex and box corrections that cannot uniquely be separated on physical grounds. As all our effective parameters are directly related to specific observables, i.e. to complete S-matrix elements, they are manifestly gauge-independent.

2.2 Predictions in the Standard Model

In order to derive the Standard Model prediction for Δy^{SC}, we have evaluated the one-loop corrections to the leptonic decay $\mathrm{W} \to \mathrm{l}\bar{\nu}_{\mathrm{l}}$, $(\mathrm{l} = \mathrm{e}, \mu, \tau)$, where the leptons and light quarks are treated as massless and the bremsstrahlung corrections integrated over the full phase space are included in the width. For the calculation of the radiative corrections we have applied standard techniques, which are e.g. reviewed in Ref. [9]. We have checked that our result for the $\mathcal{O}(\alpha)$ corrections to $\Gamma^{\mathrm{W}}_{\mathrm{l}}$ is in agreement with the result of Ref. [10], where the $\mathcal{O}(\alpha)$ corrected $\Gamma^{\mathrm{W}}_{\mathrm{l}}$ is given for arbitrary fermion masses.

We obtain for the fermion-loop contribution to Δy^{SC}

$$\begin{aligned}\Delta y^{\mathrm{SC}}_{\mathrm{ferm}} &= \mathrm{Re}\left(\frac{\Sigma^W_{\mathrm{T,ferm}}(p^2) - \Sigma^W_{\mathrm{T,ferm}}(M^2_{\mathrm{W}^\pm})}{p^2 - M^2_{\mathrm{W}^\pm}}\right)\Bigg|_{p^2=0}^{p^2\to M^2_{\mathrm{W}^\pm}} \\ &= \frac{\alpha(M_Z^2)}{16\pi s_0^2 c_0^6}\left[c_0^2(6t^2 + 3c_0^2 t - 16 c_0^4) + 6t(t^2 - c_0^4)\log\left(1 - c_0^2/t\right)\right],\end{aligned} \tag{12}$$

m_t/ GeV	$\Delta y_{\rm ferm}/10^{-3}$	$\Delta y^{\rm SC}_{\rm ferm}/10^{-3}$	$\Delta y^{\rm IB}_{\rm ferm}/10^{-3}$
120	-7.57	-7.42	-0.15
180	-6.27	-7.79	1.52
240	-5.44	-7.90	2.46

M_H/ GeV	$\Delta y_{\rm bos}/10^{-3}$	$\Delta y^{\rm SC}_{\rm bos}/10^{-3}$	$\Delta y^{\rm IB}_{\rm bos}/10^{-3}$
100	13.72	12.47	1.25
300	13.62	12.42	1.20
1000	13.61	12.41	1.20

Table 1: Fermionic and bosonic contributions to Δy, $\Delta y^{\rm SC}$, and $\Delta y^{\rm IB}$ for different values of m_t and M_H.

where $\Sigma^W_{\rm T,ferm}(p^2)$ denotes the fermion-loop contribution to the transverse part of the unrenormalized W-boson self-energy, and the shorthand $t = m_t^2/M_Z^2$ is introduced. As can be seen from (12), the fermionic contributions to $\Delta y^{\rm SC}$ are entirely given as the difference of the vacuum polarization at $p^2 = M^2_{W^\pm}$ and at $p^2 = 0$. It does not give rise to $\log(m_t)$ terms in the limit of a heavy top-quark mass. For $t \to \infty$ the fermionic contribution $\Delta y^{\rm SC}_{\rm ferm}$ is entirely given by the constant part arising from light fermion doublets,

$$\Delta y^{\rm SC}_{\rm ferm}({\rm dom}) \equiv \Delta y^{\rm SC}_{\rm ferm}\Big|_{t\to\infty} = -\frac{3\alpha(M_Z^2)}{4\pi s_0^2} \sim -8.01\times 10^{-3}, \tag{13}$$

which reflects the fact that the scale change between zero-momentum squared and $M^2_{W^\pm}$ becomes irrelevant for the contribution of an infinitely heavy top quark in the loop, i.e. the top quark decouples in the scale-change contribution. The negative sign of $\Delta y^{\rm SC}_{\rm ferm}$, according to the definition (9), shows that in analogy to the QED case the fermion loops lead to an increase of $g_{W^\pm}(M^2_{W^\pm})$ relative to $g_{W^\pm}(0)$.

The fermion-loop contribution to $\Delta y^{\rm IB}$ can directly be obtained from (10) of the previous section and formulae (19), (A.1) of Ref. [2]. We give the dominant term in the limit of a heavy top quark,

$$\Delta y^{\rm IB}_{\rm ferm}({\rm dom}) = \frac{\alpha(M_Z^2)}{8\pi s_0^2}\Big[\log(t) + 6\log(c_0^2) - \frac{1}{2} + \frac{40 s_0^2}{3} - \frac{160 s_0^4}{9}\Big], \tag{14}$$

which approximates $\Delta y^{\rm IB}_{\rm ferm}$ up to terms of $\mathcal{O}(1/m_t^2)$. Numerically we have $\Delta y^{\rm IB}_{\rm ferm}({\rm dom}) = 1.89\times 10^{-3}$ for $m_t = 180\,$GeV. In distinction to (12), the effect of isospin breaking increases logarithmically with m_t.

In Tab. 1 we give numerical results for the fermionic and bosonic contributions to Δy, $\Delta y^{\rm SC}$, and $\Delta y^{\rm IB}$ for different values of m_t and M_H. Table 1 shows that for reasonable values of the top-quark mass the asymptotic expansions (13) and (14) obtained for an infinitely heavy top quark agree with the exact results for $\Delta y^{\rm SC}_{\rm ferm}$ and $\Delta y^{\rm IB}_{\rm ferm}$ within 1×10^{-3}, justifying the terminology “dominant”.

We turn to the bosonic contributions $\Delta y^{\rm SC}_{\rm bos}$ and $\Delta y^{\rm IB}_{\rm bos}$ to Δy. They are insensitive to variations in the Higgs-boson mass M_H, as in particular they do not contain a $\log(M_H)$

term for large $M_{\rm H}$. The absence of a $\log(M_{\rm H})$ contribution in the sum $\Delta y = \Delta y^{\rm SC} + \Delta y^{\rm IB}$ was analyzed in Ref. [11] where it was shown that the heavy-Higgs limit of Δy in the SM coincides with the prediction in the Higgs-less (non-renormalizable) *massive vector-boson theory* (i.e. the SU(2)×U(1) *gauged non-linear σ-model*) which corresponds to the SM in the unitary gauge without physical Higgs field. The lack of a $\log(M_{\rm H})$ term in Δy can also be understood from the (custodial) $\mathrm{SU(2)_C}$ symmetry of the SM. Even though loop corrections do not necessarily respect this symmetry, $\mathrm{SU(2)_C}$-breaking terms generated by loops with a heavy Higgs-boson are nevertheless suppressed by a factor $1/M_{\rm H}^2$ relative to naive dimensional analysis. This result can be read off from the general effective one-loop Lagrangian [12] which quantifies the difference between the SM with a heavy Higgs boson and the massive vector-boson theory. For the $\mathrm{SU(2)_C}$-breaking parameter Δy the $1/M_{\rm H}^2$ suppression implies the absence of a $\log(M_{\rm H})$ term, in distinction from ε which corresponds to an $\mathrm{SU(2)_C}$-conserving interaction and contains a $\log(M_{\rm H})$ term, although both Δy and ε are related to dim-4 interactions. The $\mathrm{SU(2)_C}$-violating parameter Δx behaves like $\log(M_{\rm H})$, as the $M_{\rm H}^2 \log(M_{\rm H})$ term naively expected for this dim-2 interaction term is absent.

Consequently, in the limit $M_{\rm H} \to \infty$ the bosonic contribution to $\Delta y^{\rm SC}$ has the constant value

$$\begin{aligned}
\Delta y_{\rm bos}^{\rm SC}(\mathrm{dom}) \equiv \Delta y_{\rm bos}^{\rm SC}\Big|_{M_{\rm H}^2\to\infty} \\
&= \frac{\alpha(M_{\rm Z}^2)}{16\pi s_0^2}\Bigg[\frac{1}{6c_0^4}(18 - 81c_0^2 + 157c_0^4 + 296c_0^6 + 32c_0^4 s_0^2\pi^2) - 16(2+c_0^2)C_7 \\
&\quad + \frac{4}{c_0^6}(1-2c_0^2)(1+c_0^2)^2 C_6 + \frac{1}{2c_0^6}(1 + 13c_0^2 - 52c_0^4 - 28c_0^6) f_2(c_0^2) \\
&\quad - \frac{1}{2c_0^6 s_0^2}(1 + 18c_0^2 - 103c_0^4 + 94c_0^6 + 36c_0^8 - 40c_0^{10}) \log(c_0^2)\Bigg] + c_0^2\frac{3\alpha}{4\pi}. \qquad (15)
\end{aligned}$$

The definitions of the function $f_2(x)$ and the abbreviations C_6 and C_7 are given in App. B. Numerically (15) amounts to

$$\Delta y_{\rm bos}^{\rm SC}(\mathrm{dom}) = 12.41 \times 10^{-3}. \qquad (16)$$

Comparison of (16) with the values of $\Delta y_{\rm bos}^{\rm SC}$ for non-asymptotic values of $M_{\rm H}$ in Tab. 1 shows that $\Delta y_{\rm bos}^{\rm SC}(\mathrm{dom})$ is sufficiently accurate for all practical purposes. For completeness, we nevertheless give the numerically irrelevant terms of $\mathcal{O}(1/M_{\rm H}^2)$ in the appendix.

As can be seen from (13), (16) and Tab. 1, the fermionic and bosonic corrections to $\Delta y^{\rm SC}$ enter with different signs. This leads to strong cancellations in $\Delta y^{\rm SC}$ and Δy.

The analytic result for the isospin-breaking contribution $\Delta y_{\rm bos}^{\rm IB}$ can be obtained using formulae (20), (22), (A.2) of Ref. [2] and (33)–(38) of Ref. [3]. In the limit of an infinitely heavy Higgs-boson mass it reads explicitly

$$\begin{aligned}
\Delta y_{\rm bos}^{\rm IB}(\mathrm{dom}) \equiv \Delta y_{\rm bos}^{\rm IB}\Big|_{M_{\rm H}^2\to\infty} \\
&= \frac{\alpha(M_{\rm Z}^2)}{16\pi s_0^2}\Bigg[-\frac{2s_0^2}{3c_0^4}(5 + 9c_0^2 - 140c_0^4 + 278c_0^6 + 120c_0^8 + 8c_0^4\pi^2) - \frac{16}{c_0^2}(1-2c_0^2)^3 C_1
\end{aligned}$$

$$
\begin{aligned}
&- 8(1+c_0^2)^2 C_2 - 16c_0^4(2+c_0^2)C_3 - \frac{4}{c_0^6}(1+c_0^2)^2(1-2c_0^2)C_6 + 16(2+c_0^2)C_7 \\
&- (1+26c_0^2-20c_0^4-40c_0^6)f_1(c_0^2) - \frac{1}{6c_0^6}(2+23c_0^2-88c_0^4-36c_0^6)f_2(c_0^2) \\
&+ \frac{1}{6c_0^6}(2+43c_0^2-150c_0^4-60c_0^6+72c_0^8)\log(c_0^2)\Bigg] - c_0^2\frac{3\alpha}{4\pi} \\
= {}& 1.20 \times 10^{-3}. \qquad (17)
\end{aligned}
$$

The Higgs-mass dependent remainder part of $\Delta y_{\mathrm{bos}}^{\mathrm{IB}}$, which is explicitly given in App. A, is again numerically completely negligible (see Tab. 1).

It is worth noting that our investigation of Δy^{SC}, as a by-product, has lead to a compact expression for the SM one-loop result for the leptonic W-boson decay width $\Gamma_{\mathrm{l}}^{\mathrm{W}}$. According to (11), $\Gamma_{\mathrm{l}}^{\mathrm{W}}$ is expressed in terms of Δy^{SC} and $M_{\mathrm{W}^\pm}$,

$$
\Gamma_{\mathrm{l}}^{\mathrm{W}} = \frac{M_{\mathrm{W}^\pm}^3 G_\mu}{6\sqrt{2}\pi(1+\Delta y^{\mathrm{SC}})}\left(1 + c_0^2\frac{3\alpha}{4\pi}\right), \qquad (18)
$$

where the SM prediction for Δy^{SC} is given in (12), (15), (A.1), and the one for $M_{\mathrm{W}^\pm}$ in terms of Δx, Δy, ε is given in Refs. [2, 3].

2.3 Comparison with the experimental data

In Fig. 1 the theoretical result for Δy and the predictions for various contributions to Δy are compared with the experimental value of Δy, $\Delta y^{\mathrm{exp}} = (5.4 \pm 4.3) \times 10^{-3}$. The experimental value of Δy is based on the data presented for the observables $\bar{s}_{\mathrm{W}}^2$, Γ_{l}, $M_{\mathrm{W}^\pm}/M_{\mathrm{Z}}$ at the 1995 Summer Conferences [13] (see (20) below) and is obtained according to the method described in Ref. [7].

Fig. 1 demonstrates that the bosonic and also the fermionic isospin-breaking contributions, i.e. both the difference between Δy_{ferm} and $\Delta y_{\mathrm{ferm}}^{\mathrm{SC}}$ as well as the difference between Δy and $(\Delta y_{\mathrm{ferm}} + \Delta y_{\mathrm{bos}}^{\mathrm{SC}})$, are considerably smaller than the experimental error of Δy. The pure fermion-loop contribution to Δy, as previously observed [2, 3], is inconsistent with the experimental data. For full agreement with the data it is sufficient to add the bosonic scale-change contribution, $\Delta y_{\mathrm{bos}}^{\mathrm{SC}}$, to the fermion-loop result, while the bosonic isospin-breaking correction, $\Delta y_{\mathrm{bos}}^{\mathrm{IB}}$, which is about an order of magnitude smaller than $\Delta y_{\mathrm{bos}}^{\mathrm{SC}}$ (see Tab. 1), is below experimental resolution.

Combining our present result with previous ones [2, 3] on Δx and ε, we find that the approximation

$$
\Delta x \approx \Delta x_{\mathrm{ferm}}, \qquad \Delta y \approx \Delta y_{\mathrm{ferm}} + \Delta y_{\mathrm{bos}}^{\mathrm{SC}}, \qquad \varepsilon \approx \varepsilon_{\mathrm{ferm}}, \qquad (19)
$$

leads to results that deviate from the complete one-loop prediction for the effective parameters by less than the experimental errors. In other words, the experimentally significant bosonic corrections are completely contained in the effective parameter $\Delta y_{\mathrm{bos}}^{\mathrm{SC}}$ that quantifies the effect of using the low-energy input parameter G_μ for analyzing observables at the LEP energy scale. We recall that $\Delta y_{\mathrm{bos}}^{\mathrm{SC}}$, while being dependent on the non-Abelian couplings of the gauge-bosons, is totally insensitive to variations in the Higgs-boson mass.

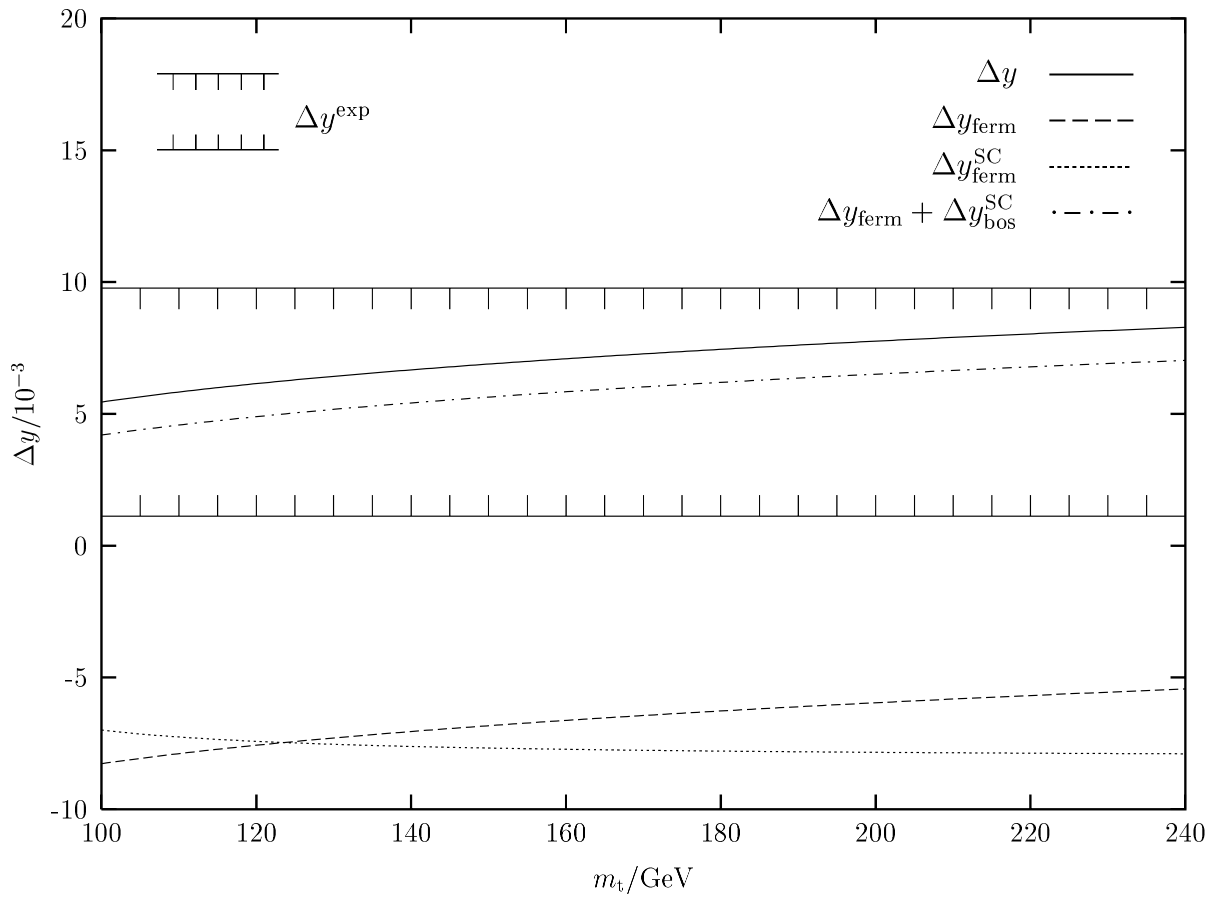

Figure 1: The one-loop SM predictions for Δy, Δy_{ferm}, $\Delta y_{\mathrm{ferm}}^{\mathrm{SC}}$, and $(\Delta y_{\mathrm{ferm}} + \Delta y_{\mathrm{bos}}^{\mathrm{SC}})$ as a function of m_{t}. The difference between the curves for Δy and $(\Delta y_{\mathrm{ferm}} + \Delta y_{\mathrm{bos}}^{\mathrm{SC}})$ corresponds to the small contribution of $\Delta y_{\mathrm{bos}}^{\mathrm{IB}}$. The experimental value of Δy, $\Delta y^{\mathrm{exp}} = (5.4 \pm 4.3) \times 10^{-3}$, is indicated by the error band.

In order to illustrate that the experimentally relevant bosonic corrections to the LEP observables and the W-boson mass are indeed just given by the contribution of $\Delta y^{\rm SC}_{\rm bos}$, we have compared in Figs. 2–5 the experimental values of the observables $\bar{s}^2_{\rm W}$, $\Gamma_{\rm l}$, $M_{\rm W^\pm}/M_{\rm Z}$ with the corresponding theoretical predictions. In Figs. 2a–5a the pure fermion-loop predictions for various values of the top-quark mass, $m_{\rm t}$, as well as the full one-loop results are compared with the experimental data. In both theoretical predictions the leading two-loop contributions of order $\mathcal{O}(\alpha_{\rm s}\alpha t)$ and $\mathcal{O}(\alpha^2 t^2)$ have also been included (see Ref. [3]). Once the bosonic scale-change contribution, $\Delta y^{\rm SC}_{\rm bos}$, is added to the fermion-loop results, as shown in Figs. 2b–5b, there is complete agreement between theory and experiment for values of the top-quark mass that are consistent with the empirical value, $m_{\rm t} = 180 \pm 12\,{\rm GeV}$ [14], obtained from the direct search. All other bosonic effects, in particular the vacuum-polarization contributions contained in $\Delta x_{\rm bos}$ and $\varepsilon_{\rm bos}$, which show a logarithmic dependence for large values of the Higgs-boson mass, are below experimental resolution for Higgs-boson masses in the perturbative regime, i.e. below $\sim 1\,{\rm TeV}$.

The experimental data used in Figs. 2–5 read [13]

$$\begin{aligned} \Gamma_{\rm l} &= 83.93 \pm 0.14\,{\rm MeV}, \\ \bar{s}^2_{\rm W}({\rm LEP}) &= 0.23186 \pm 0.00034, \\ \frac{M_{\rm W^\pm}}{M_{\rm Z}}({\rm UA2+CDF}) &= 0.8802 \pm 0.0018. \end{aligned} \tag{20}$$

We restrict our analysis to the LEP value of $\bar{s}^2_{\rm W}$. Using instead the combined LEP+SLD value, $\bar{s}^2_{\rm W} = 0.23143 \pm 0.00028$ [13], does not significantly affect our results. The theoretical predictions are based on

$$M_{\rm Z} = 91.1884 \pm 0.0022\,{\rm GeV}, \tag{21}$$

as well as the Fermi constant

$$G_\mu = 1.16639(2) \cdot 10^{-5}\,{\rm GeV}^{-2}, \tag{22}$$

the electromagnetic coupling at the Z-boson resonance,

$$\alpha(M^2_{\rm Z})^{-1} = 128.89 \pm 0.09, \tag{23}$$

which was taken from the recent updates [15] of the evaluation of the hadronic vacuum polarization, and the strong coupling

$$\alpha_{\rm s}(M^2_{\rm Z}) = 0.123 \pm 0.006, \tag{24}$$

also taken from Ref. [13].

In Figs. 2a and 2b the volume defined by the data in the three-dimensional ($M_{\rm W^\pm}/M_{\rm Z}$, $\bar{s}^2_{\rm W}$, $\Gamma_{\rm l}$)-space corresponds to the 68% C.L. (i.e. 1.9σ). The projections of the 68% C.L. volume onto the planes of the ($M_{\rm W^\pm}/M_{\rm Z}$, $\bar{s}^2_{\rm W}$, $\Gamma_{\rm l}$)-space correspond to the 83% C.L. ellipse in each plane, while the projections onto the individual axes correspond to the 94% C.L. there. In addition to the three-dimensional plots in Fig. 2, the projections in each coordinate plane are also shown in separate plots in Figs. 3–5 for better illustration. Comparison of Figs. 3a–5a with the corresponding plots of Ref. [2], where an analysis based on the 1994 data was carried out, shows that the experimental error has significantly decreased.

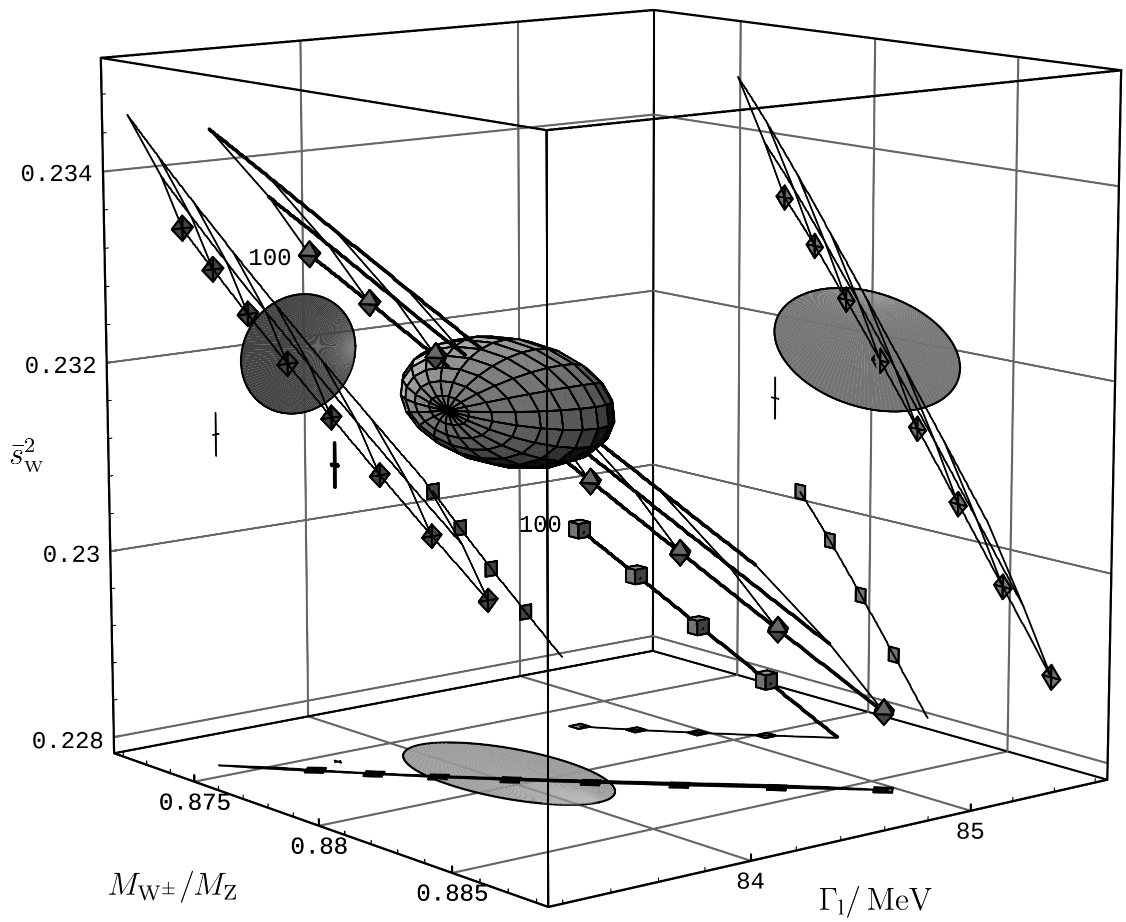

Figure 2a: Three-dimensional plot of the 68% C.L. (1.9σ) ellipsoid of the experimental data in ($M_{\mathrm{W}^\pm}/M_{\mathrm{Z}}$, $\bar{s}_{\mathrm{W}}^2$, Γ_{l})-space and comparison with the full SM prediction (connected lines) and the pure fermion-loop prediction (single line with cubes). The full SM prediction is shown for Higgs-boson masses of $M_{\mathrm{H}} = 100\,\mathrm{GeV}$ (line with diamonds), $300\,\mathrm{GeV}$, and $1\,\mathrm{TeV}$ parametrized by m_{t} ranging from 100–240 GeV in steps of 20 GeV. In the pure fermion-loop prediction the cubes also indicate steps in m_{t} of 20 GeV starting with $m_{\mathrm{t}} =$ 100 GeV. The cross outside the ellipsoid indicates the $\alpha(M_{\mathrm{Z}}^2)$-Born approximation with the corresponding error bars, which also apply to all other theoretical predictions. The projections onto the coordinate planes, which are included in the plot, are also shown in Figs. 3a–5a.

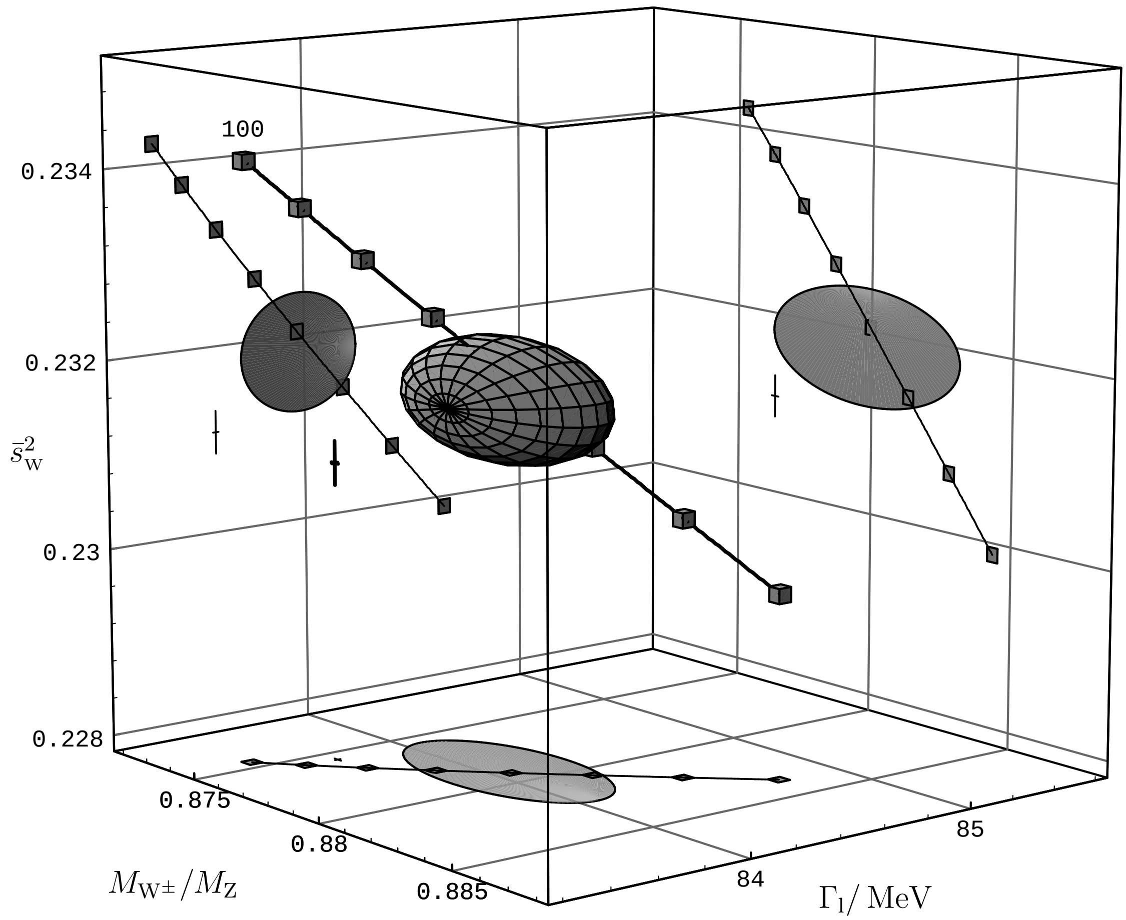

Figure 2b: Three-dimensional plot of the 68% C.L. (1.9σ) ellipsoid of the experimental data in ($M_{\mathrm{W}^\pm}/M_{\mathrm{Z}}$, $\bar{s}_{\mathrm{W}}^2$, Γ_{l})-space and comparison with the theoretical prediction obtained by combining the fermion-loop contribution with the (M_{H}-independent) bosonic correction $\Delta y_{\mathrm{bos}}^{\mathrm{SC}}$ related to the scale change from G_μ to $\Gamma_{\mathrm{l}}^{\mathrm{W}}$ (compare (9)). The theoretical prediction is parametrized by m_{t} ranging from 100–240 GeV in steps of 20 GeV. The projections onto the coordinate planes, which are included in the plot, are also shown in Figs. 3b–5b.

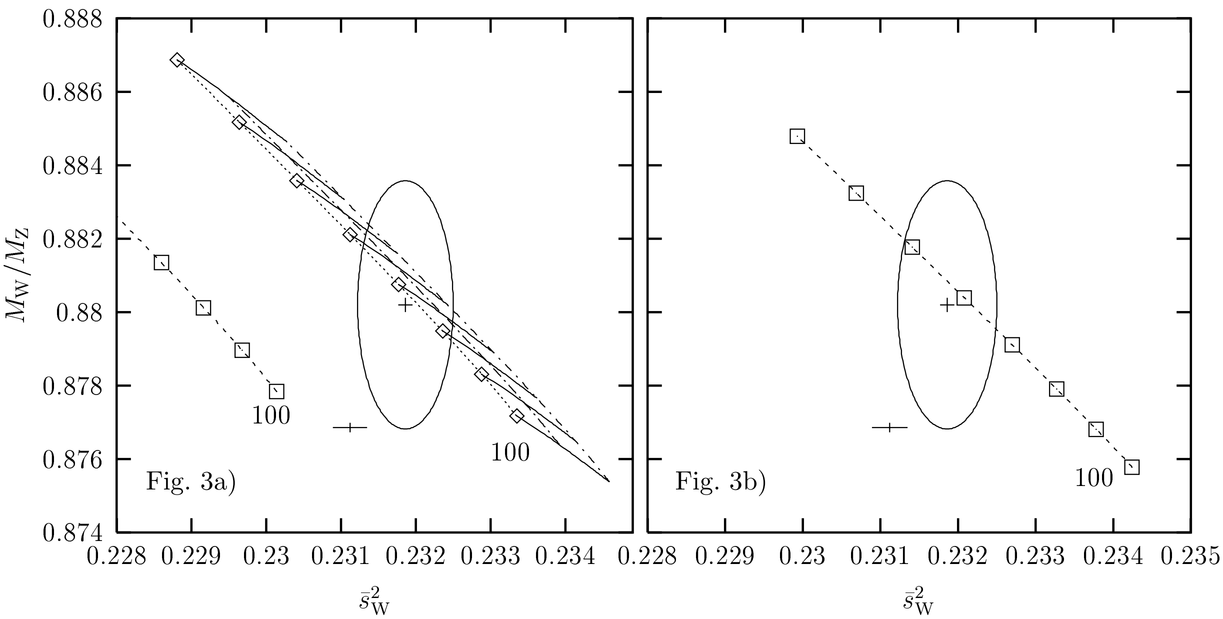

Figure 3: Projection of the 68% C.L. (1.9σ) volume of the experimental data in ($M_{\mathrm{W}^\pm}/M_{\mathrm{Z}}$, $\bar{s}^2_{\mathrm{W}}$, Γ_{l})-space onto the ($\bar{s}^2_{\mathrm{W}}$, $M_{\mathrm{W}^\pm}/M_{\mathrm{Z}}$)-plane. In Fig. 3a the pure fermion-loop prediction is indicated by the single line, the squares denote steps of 20 GeV in m_{t}. The full SM prediction is shown for Higgs-boson masses of $M_{\mathrm{H}} = 100\,\mathrm{GeV}$ (dotted with diamonds), 300 GeV (long-dashed-dotted) and 1 TeV (short-dashed-dotted) parametrized by m_{t} ranging from 100–240 GeV in steps of 20 GeV. Fig. 3b shows the theoretical prediction obtained by combining the fermion-loop contribution with the (M_{H}-independent) bosonic correction $\Delta y^{\mathrm{SC}}_{\mathrm{bos}}$.

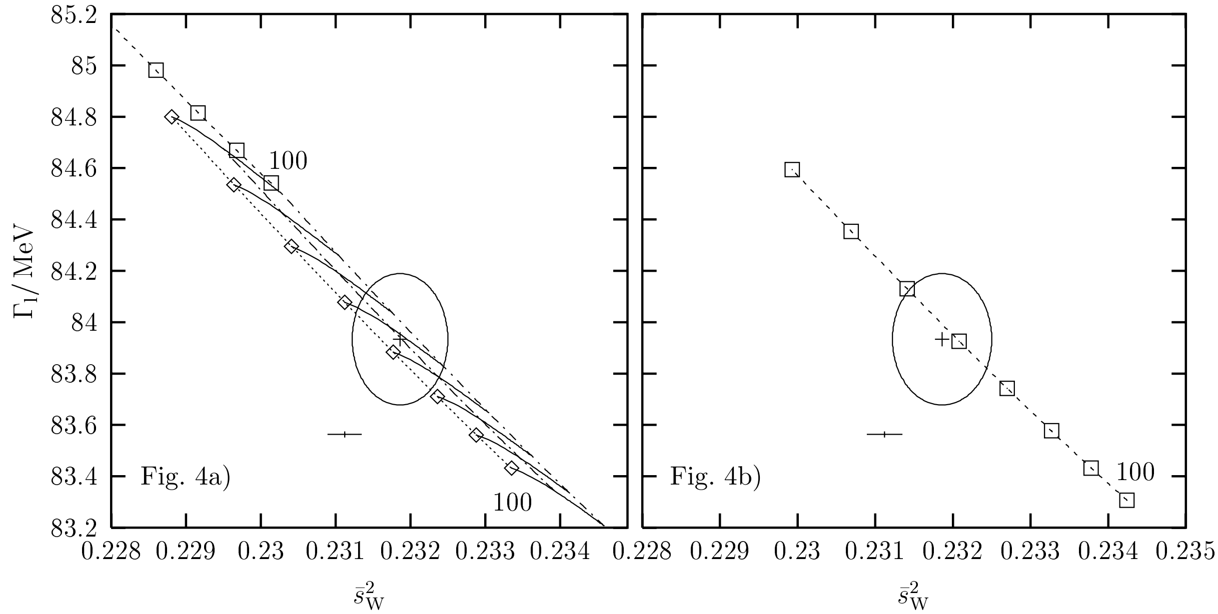

Figure 4: Same signature as Fig. 3, but for the ($\bar{s}^2_{\mathrm{w}}$, Γ_{l})-plane.

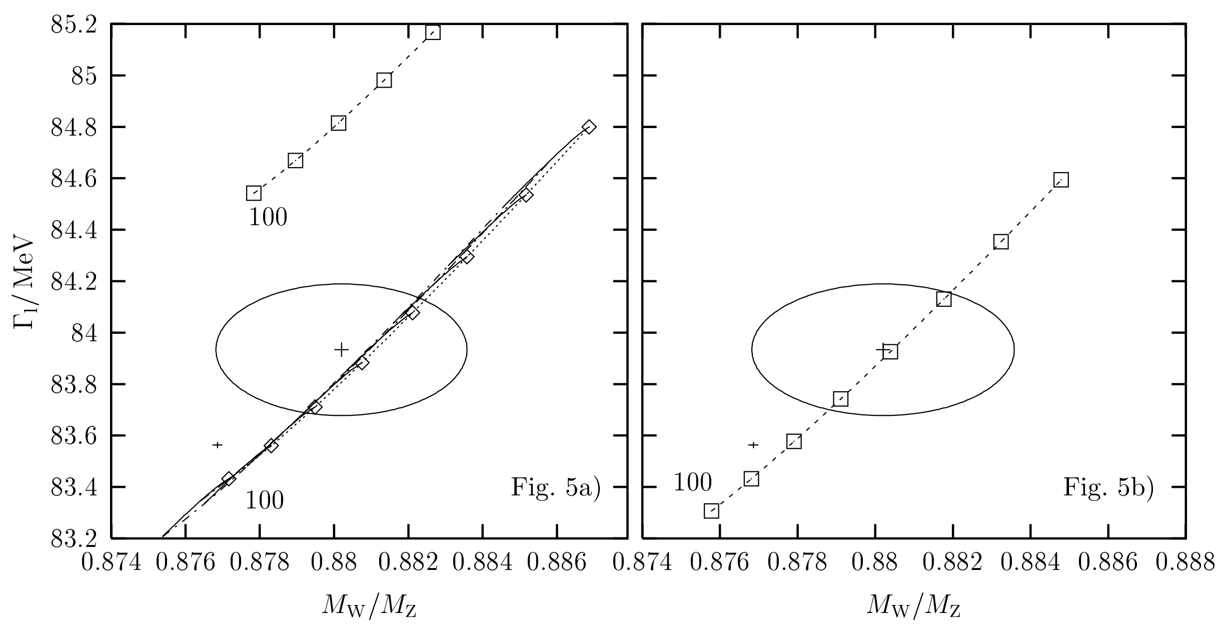

Figure 5: Same signature as Fig. 3, but for the ($M_{\mathrm{W}^\pm}/M_{\mathrm{Z}}$, Γ_{l})-plane.

The fermion-loop predictions in Figs. 2a–5a are based on the approximation

$$\Delta x \approx \Delta x_{\rm ferm}, \qquad \Delta y \approx \Delta y_{\rm ferm}, \qquad \varepsilon \approx \varepsilon_{\rm ferm}. \tag{25}$$

For $m_{\rm t} = 180\,{\rm GeV}$ the pure fermion-loop predictions at one loop read

$$\begin{aligned} \bar{s}^2_{\rm W,ferm} &= 0.22747 \mp 0.00023, \\ \left(\frac{M_{\rm W^\pm}}{M_{\rm Z}}\right)_{\rm ferm} &= 0.88358 \pm 0.00013, \\ \Gamma_{\rm l,ferm} &= 85.299 \pm 0.012\,{\rm MeV}, \end{aligned} \tag{26}$$

which deviate from the experimental values by -13σ, 1.9σ and 9.8σ, respectively.

The uncertainties of the theoretical predictions are dominated by the error of $\alpha(M_{\rm Z}^2)$ given in (23). In Figs. 2–5 the $\alpha(M_{\rm Z}^2)$-Born approximation,

$$s_0^2 = 0.23112 \mp 0.00023, \quad c_0 = 0.87686 \pm 0.00013, \quad \Gamma_{\rm l}^{(0)} = 83.563 \pm 0.012\,{\rm MeV}, \tag{27}$$

is also indicated for completeness. The error bars shown for the $\alpha(M_{\rm Z}^2)$-Born approximation of course also apply to the other theoretical predictions. The $\alpha(M_{\rm Z}^2)$-Born approximation corresponds to a deviation of -2.2σ, -1.9σ and -2.6σ, respectively, from the experimental data. The fact that the values in (27) are closer to the empirical data and the full SM predictions than the fermion-loop prediction (26) is a consequence of the cancellation between fermionic and bosonic contributions in the single parameter $\Delta y^{\rm SC}$ as displayed in Tab. 1.

The comparison of the full SM predictions with the data in Figs. 2a–5a also illustrates in how far the data are sensitive to variations in the Higgs-boson mass. For fixed values of $m_{\rm t} \sim 180\,{\rm GeV}$ the intersection of the 68% C.L. (1.9σ) volume with the SM prediction allows for Higgs masses which span the full range from the experimental lower bound of $\sim 60\,{\rm GeV}$ to about 1 TeV. It should also be noted that in the direction in three-dimensional space in which the $M_{\rm H}$-dependence (for fixed $m_{\rm t}$) is sizable also the uncertainty in the theoretical predictions due to the error in $\alpha(M_{\rm Z}^2)$ is large.

3 Radiative corrections in the $\Gamma_{\rm l}^{\rm W}$-scheme

In the previous section, using the framework of an effective Lagrangian and the specific parametrization of the radiative corrections in terms of Δx, Δy, and ε, we have identified the experimentally relevant bosonic corrections in the analysis of the precision data with the contribution of the single effective parameter $\Delta y^{\rm SC}_{\rm bos}$. In the present section we will formulate this observation in a way that is independent of any specific parametrization and that makes the physical interpretation of those bosonic corrections that are in fact tested in current precision experiments more transparent.

As shown in the last section, the parameter $\Delta y^{\rm SC}_{\rm bos}$ expresses the effect of using the low-energy quantity G_μ as input parameter for the analysis of the LEP observables. We will now demonstrate that these large bosonic corrections could indeed completely be avoided by expressing the theoretical predictions for the observables $\bar{s}^2_{\rm W}$, $\Gamma_{\rm l}$, $M_{\rm W^\pm}/M_{\rm Z}$ in terms of

appropriate input parameters being defined at the scale of the vector-boson masses, namely by using the W-boson width $\Gamma_{\mathrm{l}}^{\mathrm{W}}$ instead of the Fermi constant G_μ as input parameter.

In the language of the effective Lagrangian $\mathcal{L}_{\mathrm{C}}$ given in (4) the use of the input quantity $\Gamma_{\mathrm{l}}^{\mathrm{W}}$ instead of G_μ means that the charged-current coupling in (4) is identified with $g_{\mathrm{W}^\pm}(M_{\mathrm{W}^\pm}^2)$ defined via the W-boson width $\Gamma_{\mathrm{l}}^{\mathrm{W}}$ (see (6)) rather than with $g_{\mathrm{W}^\pm}(0)$ defined via muon decay (see (5)). With this identification the transition between $g_{\mathrm{W}^\pm}(0)$ and $g_{\mathrm{W}^\pm}(M_{\mathrm{W}^\pm}^2)$, and accordingly the contribution of Δy^{SC}, does not occur. The radiative corrections to the observables $\bar{s}_{\mathrm{W}}^2$, Γ_{l}, and $M_{\mathrm{W}^\pm}/M_{\mathrm{Z}}$ are completely contained in the parameters Δx, Δy^{IB}, and ε, in which SM corrections beyond fermion loops do not give rise to significant contributions.

In this "$\Gamma_{\mathrm{l}}^{\mathrm{W}}$-scheme" the lowest-order values $\hat{s}_0^2$, $\hat{c}_0$, and $\hat{\Gamma}_{\mathrm{l}}^{(0)}$ of the observables are given in terms of the input quantities $\alpha(M_{\mathrm{Z}}^2)$, M_{Z}, and $\Gamma_{\mathrm{l}}^{\mathrm{W}}$ as

$$\frac{\hat{s}_0^2}{\hat{c}_0} \equiv \frac{\alpha(M_{\mathrm{Z}}^2)M_{\mathrm{Z}}}{12\Gamma_{\mathrm{l}}^{\mathrm{W}}}\left(1+c_0^2\frac{3\alpha}{4\pi}\right), \qquad \hat{c}_0^2 \equiv (1-\hat{s}_0^2), \tag{28}$$

and

$$\hat{\Gamma}_{\mathrm{l}}^{(0)} = \frac{\alpha(M_{\mathrm{Z}}^2)M_{\mathrm{Z}}}{48\hat{s}_0^2\hat{c}_0^2}\left[1+(1-4\hat{s}_0^2)^2\right]\left(1+\frac{3\alpha}{4\pi}\right). \tag{29}$$

The relations between the observables and the effective parameters x, y^{IB}, and ε read

$$\begin{aligned}
\bar{s}_{\mathrm{W}}^2\left(1-\bar{s}_{\mathrm{W}}^2\right) &= \frac{\hat{s}_0^2}{\hat{c}_0}\frac{M_{\mathrm{W}^\pm}^3}{M_{\mathrm{Z}}^3}\frac{y^{\mathrm{IB}}-2\hat{s}_0^2\delta}{x+2\hat{s}_0^2\delta}(1-\varepsilon+\delta)\frac{1}{\left(1+\frac{\bar{s}_{\mathrm{W}}^2}{1-\bar{s}_{\mathrm{W}}^2}(\varepsilon-\delta)\right)},\\
\frac{M_{\mathrm{W}^\pm}^2}{M_{\mathrm{Z}}^2} &= \left(1-\bar{s}_{\mathrm{W}}^2\right)\left(x+2\hat{s}_0^2\delta\right)\left(1+\frac{\bar{s}_{\mathrm{W}}^2}{1-\bar{s}_{\mathrm{W}}^2}(\varepsilon-\delta)\right),\\
\Gamma_{\mathrm{l}} &= \frac{\Gamma_{\mathrm{l}}^{\mathrm{W}}M_{\mathrm{Z}}^3}{4M_{\mathrm{W}^\pm}^3}\left[1+\left(1-4\bar{s}_{\mathrm{W}}^2\right)^2\right]\frac{x+2\hat{s}_0^2\delta}{y^{\mathrm{IB}}-2\hat{s}_0^2\delta}\left(1+s_0^2\frac{3\alpha}{4\pi}\right).
\end{aligned} \tag{30}$$

The small parameter δ ($\delta \sim 10^{-4}$ in the SM), which describes parity violation in the photonic coupling at the Z-boson mass scale, has been defined in Ref. [3]. The relations (30) are simply obtained from eqs. (16) of Ref. [3], where the observables are expressed in terms of the input parameters $\alpha(M_{\mathrm{Z}}^2)$, M_{Z}, and G_μ, by the replacement

$$G_\mu = y^{\mathrm{SC}}\Gamma_{\mathrm{l}}^{\mathrm{W}}\frac{6\sqrt{2}\pi}{M_{\mathrm{W}^\pm}^3}\left(1+c_0^2\frac{3\alpha}{4\pi}\right)^{-1}, \tag{31}$$

which explicitly illustrates that the contribution of Δy^{SC} is absorbed by introducing the "large-scale" quantity $\Gamma_{\mathrm{l}}^{\mathrm{W}}$. Linearizing (30) in Δx, Δy^{IB}, ε, and δ yields

$$\begin{aligned}
\bar{s}_{\mathrm{W}}^2 &= \hat{s}_0^2\left[1+\frac{\hat{c}_0^2}{2-\hat{s}_0^2}\Delta x+\frac{2\hat{c}_0^2}{2-\hat{s}_0^2}\Delta y^{\mathrm{IB}}+\frac{3\hat{s}_0^2-2}{2-\hat{s}_0^2}\varepsilon+(\hat{c}_0^2-\hat{s}_0^2)\delta\right],\\
\frac{M_{\mathrm{W}^\pm}}{M_{\mathrm{Z}}} &= \hat{c}_0\left[1+\frac{\hat{c}_0^2}{2-\hat{s}_0^2}\Delta x-\frac{\hat{s}_0^2}{2-\hat{s}_0^2}\Delta y^{\mathrm{IB}}+\frac{2\hat{s}_0^2}{2-\hat{s}_0^2}\varepsilon\right],\\
\Gamma_{\mathrm{l}} &= \hat{\Gamma}_{\mathrm{l}}^{(0)}\Bigg[1-\frac{2}{(2-\hat{s}_0^2)\left[1+(1-4\hat{s}_0^2)^2\right]}\Big((1-2\hat{s}_0^2-4\hat{s}_0^4)(\Delta x+2\Delta y^{\mathrm{IB}})\\
&\qquad -2\hat{s}_0^2(1-10\hat{s}_0^2)\varepsilon-8\hat{s}_0^4(2-\hat{s}_0^2)\delta\Big)\Bigg].
\end{aligned} \tag{32}$$

	G_μ−scheme		$\Gamma_{\rm l}^{\rm W}$−scheme		
	ferm. corr.	bos. corr.	ferm. corr.	bos. corr.	exp. error
$\frac{\Delta\bar{s}^2_{\rm W}}{\bar{s}^2_{\rm W}}/10^{-3}$	−15.8	16.3	11.0	1.3	1.5
$\frac{\Delta M_{\rm W^\pm}}{M_{\rm W^\pm}}/10^{-3}$	7.7	− 1.6	3.7	0.6	2.0
$\frac{\Delta\Gamma_{\rm l}}{\Gamma_{\rm l}}/10^{-3}$	20.8	−14.3	− 1.8	−1.7	1.7

Table 2: Relative size of the SM fermionic and bosonic one-loop corrections to the observables $\bar{s}^2_{\rm W}$, $M_{\rm W^\pm}$, and $\Gamma_{\rm l}$ in the G_μ-scheme (input parameters G_μ, $M_{\rm Z}$, and $\alpha(M^2_{\rm Z})$) and in the simulated $\Gamma_{\rm l}^{\rm W}$-scheme (input parameters $\Gamma_{\rm l}^{\rm W} = 226.3\,{\rm MeV}$, $M_{\rm Z}$, and $\alpha(M^2_{\rm Z})$) for $m_{\rm t} = 180\,{\rm GeV}$ and $M_{\rm H} = 300\,{\rm GeV}$. The relative experimental error of the observables is also indicated.

The relations (32) could in principle be used for a data analysis of the observables $\bar{s}^2_{\rm W}$, $\Gamma_{\rm l}$, and $M_{\rm W^\pm}/M_{\rm Z}$ in the $\Gamma_{\rm l}^{\rm W}$-scheme, i.e. with $\alpha(M^2_{\rm Z})$, $M_{\rm Z}$, and $\Gamma_{\rm l}^{\rm W}$ as experimental input quantities. Assuming (hypothetically) the same experimental accuracy as in the "G_μ-scheme" (input parameters $\alpha(M^2_{\rm Z})$, $M_{\rm Z}$, and G_μ) and an experimental value of $\Gamma_{\rm l}^{\rm W}$ being in agreement with the SM prediction, a consistent description of the data in the $\Gamma_{\rm l}^{\rm W}$-scheme would be possible by solely including the pure fermion-loop predictions in the effective parameters.

At present a data analysis using the $\Gamma_{\rm l}^{\rm W}$-scheme would of course not be sensible owing to the large experimental error in the determination of the W-boson width. From Ref. [16] we have $\Gamma_{\rm T}^{\rm W,exp} = (2.08 \pm 0.07)\,{\rm GeV}$ for the total decay width of the W-boson and $(10.7 \pm 0.5)\%$ for the leptonic branching ratio. Adding the errors quadratically yields $\Gamma_{\rm l}^{\rm W,exp} = (223 \pm 13)\,{\rm MeV}$ showing that the experimental error in $\Gamma_{\rm l}^{\rm W,exp}$ at present is more than an order of magnitude larger than the error in the leptonic Z-boson width (see (20)) and obviously much larger than the one in G_μ (see (22)).

Even though a precise experimental input value for $\Gamma_{\rm l}^{\rm W}$ is not available it is nevertheless instructive to simulate the analysis in the $\Gamma_{\rm l}^{\rm W}$-scheme by using the theoretical SM value for $\Gamma_{\rm l}^{\rm W}$ as hypothetical input parameter for evaluating (32). For the choice of $m_{\rm t} = 180\,{\rm GeV}$ and $M_{\rm H} = 300\,{\rm GeV}$ one obtains $\Gamma_{\rm l}^{\rm W} = 226.3\,{\rm MeV}$ as theoretical value of $\Gamma_{\rm l}^{\rm W}$ in the SM. One should note that our procedure here is technically analogous to commonly used parametrizations of radiative corrections where, for instance in the on-shell scheme (see e.g. Ref. [9]), the corrections are expressed in terms of the W-boson mass $M_{\rm W^\pm}$, while in an actual evaluation $M_{\rm W^\pm}$ is substituted by its theoretical SM value in terms of $\alpha(M^2_{\rm Z})$, $M_{\rm Z}$, and G_μ.

In order to illustrate the fact that the replacement of the input quantity G_μ by $\Gamma_{\rm l}^{\rm W}$ indeed strongly affects the relative size of the fermionic and bosonic contributions entering each observable, we have given in Tab. 2 the relative values of the SM one-loop fermionic and bosonic corrections to the observables $\bar{s}^2_{\rm W}$, $M_{\rm W^\pm}$, and $\Gamma_{\rm l}$ in the G_μ-scheme and in the simulated $\Gamma_{\rm l}^{\rm W}$-scheme based on the input value $\Gamma_{\rm l}^{\rm W} = 226.3\,{\rm MeV}$. The size of the radiative corrections in the two schemes is compared with the relative experimental error of the

observables (see (20)). Table 2 shows that in the G_μ-scheme the bosonic corrections to $\bar{s}^2_{\mathrm{W}}$ and Γ_{l} are quite sizable and considerably larger than the experimental error. In the (simulated) $\Gamma^{\mathrm{W}}_{\mathrm{l}}$-scheme, on the other hand, these corrections are smaller by an order of magnitude and have about the same size as the experimental error. The bosonic contributions to $M_{\mathrm{W}^\pm}$ are smaller than the experimental error in both schemes. It can furthermore be seen in Tab. 2 that the cancellation between fermionic and bosonic corrections related to the scale change is not present in the $\Gamma^{\mathrm{W}}_{\mathrm{l}}$-scheme.

The explicit values for the pure fermion-loop predictions of the observables at one-loop order in the simulated $\Gamma^{\mathrm{W}}_{\mathrm{l}}$-scheme read

$$\bar{s}^2_{\mathrm{W,ferm}} = 0.23154, \qquad \left(\frac{M_{\mathrm{W}^\pm}}{M_{\mathrm{Z}}}\right)_{\mathrm{ferm}} = 0.8813, \qquad \Gamma_{\mathrm{l,ferm}} = 84.06\,\mathrm{MeV}. \tag{33}$$

Comparison with the experimental values of the observables given in (20) shows that there is indeed no significant deviation between the pure fermion-loop predictions in the simulated $\Gamma^{\mathrm{W}}_{\mathrm{l}}$-scheme and the data, i.e. they agree within one standard deviation. This has to be contrasted to the situation in the G_μ-scheme, where the pure fermion-loop predictions differ from the data by several standard deviations (see (26) and Fig. 2a–5a).

In summary, we have demonstrated that after replacing the low-energy quantity G_μ by the high-energy observable $\Gamma^{\mathrm{W}}_{\mathrm{l}}$ in the theoretical predictions for the observables $\bar{s}^2_{\mathrm{W}}$, $M_{\mathrm{W}^\pm}/M_{\mathrm{Z}}$, and Γ_{l}, no corrections beyond fermion loops are required in order to consistently describe the data. Although at present, due to the large experimental error in $\Gamma^{\mathrm{W}}_{\mathrm{l}}$, the so-defined $\Gamma^{\mathrm{W}}_{\mathrm{l}}$-scheme is of no practical use for analyzing these precision data, from a theoretical point of view it shows that the only bosonic corrections of significant magnitude are such that they can completely be absorbed by the introduction of the quantity $\Gamma^{\mathrm{W}}_{\mathrm{l}}$. It is obvious that all results of this section do not depend on any specific parametrization, such as the description via Δx, Δy^{IB}, ε, chosen for analyzing the data. They only rely on the set of physical observables chosen as input parameters.

4 Conclusions

It is by now a well established fact that the experimental data on the leptonic LEP1 observables Γ_{l}, $\bar{s}^2_{\mathrm{W}}$ and the W-boson mass $M_{\mathrm{W}^\pm}$ are sensitive to radiative corrections beyond pure fermion loops. In this paper we have investigated in detail which standard electroweak bosonic loop corrections are in fact tested by the experiments.

Starting from an analysis of the radiative corrections in terms of the effective parameters Δx, Δy, and ε, which quantify different sources of SU(2) violation in an effective Lagrangian, we have shown that the bosonic corrections needed for an agreement between the SM predictions and the current precision data can be identified as an effect of the transition from the low-energy process muon decay to the LEP observables. In the framework of the effective Lagrangian all experimentally significant bosonic corrections are contained in the single effective parameter Δy^{SC} that quantifies the difference between the charged-current coupling $g_{\mathrm{W}^\pm}(0)$ defined via the low-energy process muon decay and the charged-current coupling $g_{\mathrm{W}^\pm}(M^2_{\mathrm{W}^\pm})$ at the W-boson mass shell. This fact has been demonstrated not only at the level of the effective parameters, but also by confronting theory and experiment for the observables Γ_{l}, $\bar{s}^2_{\mathrm{W}}$, and $M_{\mathrm{W}^\pm}$ themselves.

As a consequence of these investigations, a simple physical interpretation of those bosonic corrections that are resolved by the current precision experiments can be given. They are precisely the ones that appear when W-boson decay is expressed in terms of the input parameter G_μ and can therefore directly be related to the set of physical observables chosen as input parameters for the data analysis. Upon introducing the high-energy quantity $\Gamma_{\rm l}^{\rm W}$ ($\Gamma_{\rm l}^{\rm W}$-scheme) as input parameter instead of G_μ (G_μ-scheme), the significant bosonic corrections are completely absorbed when analyzing the high-energy observables $\bar{s}^2_{\rm W}$, $\Gamma_{\rm l}$, and $M_{\rm W^\pm}/M_{\rm Z}$. Since the usefulness of $\Gamma_{\rm l}^{\rm W}$ as experimental input parameter is limited at present due to the large experimental error of the W-boson width, we have demonstrated this fact by invoking the SM theoretical value of $\Gamma_{\rm l}^{\rm W}$ as input. Indeed, no further corrections beyond fermion loops are needed in this case in order to achieve agreement with the data within one standard deviation.

It is amusing to note that the precision data collected at LEP, i.e. for a neutral-current process at the Z-boson resonance, provide a test of just those bosonic radiative corrections that are associated with the charged-current process of W-boson decay. While the experimentally significant bosonic corrections are insensitive to variations in the Higgs-boson mass, they provide a highly non-trivial, even though indirect, test of the non-Abelian gauge structure of the electroweak theory.

Acknowledgement

The authors thank Masaaki Kuroda for interesting discussions. One of the authors (D.S.) thanks the Max Planck Institut, Werner Heisenberg Institut für Physik, München, for hospitality while part of the present work was done.

Appendix

A Remainders of $\Delta y^{\rm SC}_{\rm bos}$ and $\Delta y^{\rm IB}_{\rm bos}$

In Sect. 2 we have split the parameters $\Delta y^{\rm SC,IB}_{\rm bos}$ into dominant parts $\Delta y^{\rm SC,IB}_{\rm bos}$(dom) and remainder parts containing the $M_{\rm H}$-dependence, which is numerically completely negligible. The remainder parts read explicitly

$$\begin{aligned}\Delta y^{\rm SC}_{\rm bos}({\rm rem}) = \frac{\alpha(M_{\rm Z}^2)}{32\pi c_0^6 s_0^2}\Bigg[&-\frac{c_0^2}{3}(47c_0^4-21c_0^2h+6h^2)\\ &+\frac{1}{c_0^2-h}(4c_0^8-22c_0^6h+17c_0^4h^2-6c_0^2h^3+h^4)\log\left(\frac{c_0^2}{h}\right)\\ &+\frac{1}{4c_0^2-h}h(28c_0^6-20c_0^4h+7c_0^2h^2-h^3)f_2\left(\frac{c_0^2}{h}\right)\Bigg],\end{aligned} \tag{A.1}$$

$$\Delta y^{\rm IB}_{\rm bos}({\rm rem}) = \frac{\alpha(M_{\rm Z}^2)}{96\pi s_0^2}\Bigg[-\frac{4s_0^2h}{c_0^4}(3c_0^2-h-c_0^2h)$$

$$+\left(10-18\frac{h}{c_0^2}+9\frac{h^2}{c_0^4}-2\frac{h^3}{c_0^6}\right)\log\left(\frac{h}{c_0^2}\right)-(10-18h+9h^2-2h^3)\log(h)$$
$$-\left(36-32\frac{h}{c_0^2}+13\frac{h^2}{c_0^4}-2\frac{h^3}{c_0^6}\right)\frac{h}{4c_0^2-h}f_2\left(\frac{c_0^2}{h}\right)$$
$$+(36-32h+13h^2-2h^3)\frac{h}{4-h}f_2\left(\frac{1}{h}\right)\Bigg], \tag{A.2}$$

where the shorthand $h = M_\mathrm{H}^2/M_\mathrm{Z}^2$ is used. By definition, $\Delta y_\mathrm{bos}^\mathrm{SC,IB}(\mathrm{rem})$ approach asymptotically zero for $h \to \infty$.

B Auxiliary functions

Here we list the explicit expressions for the auxiliary functions which have been used in Sect. 2 and App. A for the explicit formulae of the bosonic contributions to Δy^SC and Δy^IB. As defined in Ref. [2], $f_{1,2}(x)$ are given by

$$f_1(x) = \mathrm{Re}\left[\beta_x \log\left(\frac{\beta_x-1}{\beta_x+1}\right)\right], \quad \text{with } \beta_x = \sqrt{1-4x+i\epsilon},$$
$$f_2(x) = \mathrm{Re}\left[\beta_x^* \log\left(\frac{1-\beta_x^*}{1+\beta_x^*}\right)\right]. \tag{B.3}$$

Furthermore, some scalar one-loop three-point integrals have been abbreviated by

$$C_1 = M_\mathrm{Z}^2\,\mathrm{Re}\left[C_0(0,0,M_\mathrm{Z}^2,0,M_\mathrm{Z},0)\right] = -\frac{\pi^2}{12} = -0.8225,$$
$$C_2 = M_\mathrm{Z}^2\,\mathrm{Re}\left[C_0(0,0,M_\mathrm{Z}^2,0,M_\mathrm{W},0)\right] = \frac{\pi^2}{6} - \mathrm{Re}\left[\mathrm{Li}_2\left(1+\frac{1}{c_0^2}\right)\right] = -0.8037,$$
$$C_3 = M_\mathrm{Z}^2\,\mathrm{Re}\left[C_0(0,0,M_\mathrm{Z}^2,M_\mathrm{W},0,M_\mathrm{W})\right] = \mathrm{Re}\left[\log^2\left(\frac{i\sqrt{4c_0^2-1}-1}{i\sqrt{4c_0^2-1}+1}\right)\right] = -1.473,$$
$$C_6 = c_0^2 M_\mathrm{Z}^2\,\mathrm{Re}\left[C_0(0,0,M_{\mathrm{W}^\pm}^2,0,M_\mathrm{Z},0)\right] = \frac{\pi^2}{6} - \mathrm{Re}\left[\mathrm{Li}_2\left(1+c_0^2\right)\right] = -0.8067,$$
$$C_7 = c_0^2 M_\mathrm{Z}^2\,\mathrm{Re}\left[C_0(0,0,M_{\mathrm{W}^\pm}^2,M_{\mathrm{W}^\pm},0,M_\mathrm{Z})\right]$$
$$= -\log\left[\frac{1}{2}\left(1+i\sqrt{4c_0^2-1}\right)\right]\log\left[\frac{1}{2}\left(1-i\sqrt{4c_0^2-1}\right)\right] = -0.9466, \tag{B.4}$$

with the dilogarithm

$$\mathrm{Li}_2(x) = -\int_0^x \frac{dt}{t}\log(1-t), \qquad -\pi < \mathrm{arc}(1-x) < \pi. \tag{B.5}$$

The first three arguments of the C_0-function label the external momenta squared, the last three the inner masses of the corresponding vertex diagram.

References

[1] G. Gounaris, D. Schildknecht, *Z. Phys.* **C40** (1988) 447.

[2] S. Dittmaier, K. Kolodziej, M. Kuroda, and D. Schildknecht, *Nucl. Phys.* **B426** (1994) 249, E: **B446** (1995) 334.

[3] S. Dittmaier, M. Kuroda, and D. Schildknecht, *Nucl. Phys.* **B448** (1995) 3.

[4] V.A. Novikov, L.B. Okun, A.N. Rozanov and M.I. Vysotsky, *Mod. Phys. Lett.* **A9** (1994) 2641.

[5] P. Gambino and A. Sirlin, *Phys. Rev. Lett.* **73** (1994) 621.

[6] Z. Hioki, *Int. J. Mod. Phys.* **A10** (1995) 3803;
Z. Hioki, TOKUSHIMA 95-04, hep-ph/9510269.

[7] M. Bilenky, K. Kolodziej, M. Kuroda, and D. Schildknecht, *Phys. Lett.* **B319** (1993) 319.

[8] G. Altarelli, R. Barbieri, and F. Caravaglios, *Nucl. Phys.* **B405** (1993) 3.

[9] A. Denner, *Fortschr. Phys.* **41** (1993) 307.

[10] A. Denner and T. Sack, *Z. Phys.* **C46** (1990) 653.

[11] S. Dittmaier, C. Grosse-Knetter and D. Schildknecht, *Z. Phys.* **C67** (1995) 109.

[12] M.J. Herrero and E. Ruiz Morales, *Nucl. Phys.* **B418** (1994) 431;
S. Dittmaier and C. Grosse-Knetter, BI-TP 95/10, hep-ph/9505266, to appear in *Nucl. Phys.* **B**.

[13] LEP Electroweak Working Group, Data presented at the 1995 Summer Conferences, LEPEWWG/95-02.

[14] F. Abe et al., CDF collaboration, *Phys. Rev. Lett.* **74** (1995) 2626,
S. Abachi et al., DØ collaboration, *Phys. Rev. Lett.* **74** (1995) 2632.

[15] H. Burkhardt and B. Pietrzyk, *Phys. Lett.* **B356** (1995) 398;
S. Eidelman and F. Jegerlehner, *Z. Phys.* **C67** (1995) 585.

[16] M. Aguilar-Benitez et al., Particle Data Group, *Phys. Rev.* **D50** (1994) 1173.